NOx reduction based on N2 dilution in a swirled-stabilized magnesium flame

Adeline Andrieu, Olivier Allgaier, Gontrand Leyssens, Cornelius Schönnenbeck, Jean-François Brilhac, Alain Brillard, Valérie Tschamber

NOx reduction based on N_2 dilution in a swirled-stabilized magnesium flame

Adeline Andrieu, Olivier Allgaier, Gontrand Leyssens, Cornelius Schönnenbeck, Jean-François Brilhac[1], Alain Brillard, Valérie Tschamber

LGRE UHA UR 2334, Université de Haute-Alsace, 68093 Mulhouse, France

Abstract

New sources of clean energy with reduced greenhouse gas emissions must be considered because of global warming. Among these alternative sources, metal fuels such as aluminum or magnesium are promising. The present study focuses on the impacts of an air dilution by N_2 and of the equivalence ratio on the amount of nitrogen oxides (NOx) produced by a swirled-stabilized magnesium flame. A polydispersed aerosol of pure magnesium in the size fraction 50-70 µm was injected in the combustion chamber. Different air-fuel ratios – from 0.14 to 1.0 – were obtained by changing the mass flowrate of the injected fuel. Thermocouples and a pyrometer were implemented to monitor the gas and flame temperatures. On-line paramagnetic analyzers were used to measure the oxygen (O_2) and NOx concentrations. For each dilution condition (0, 30 and 50%), the NOx mole fraction versus the equivalence ratio follows a parabolic shape. The amount of NOx first increases when increasing the air-fuel ratio as the power dissipated by the flame increases, leading to the rise of the gas temperature. For the highest air-fuel ratios, the NOx production is disfavored in the rich mixture. The maximal NOx emissions are shifted to higher equivalent ratios when increasing the dilution level and it decreases by a factor 2 with a dilution of 50%, for a constant value of the air-fuel ratio. The gas temperature in the flame decreases due to the N_2 dilution. The NOx emissions become negligible for an equivalence ratio of 1 at a 50% dilution. Nevertheless, under the tested experimental conditions, the level of NOx never exceeded 7 gNOx/kWh, which is lower than the maximal value of NOx emissions from a gasoline engine.

[1] Corresponding author.
Email address: jean-francois.brilhac@uha.fr (J.-F. Brilhac)

Keywords. Magnesium combustion; NOx emissions; N_2 dilution; equivalence ratio

1. Introduction

The combustion of metal elements can be considered to produce a clean, renewable and carbon-free energy. Metal powders such as magnesium or aluminum are indeed an energy source for the future, as energetic as fossil resources and without CO_2 emissions [1,2]. In addition, the metal oxide particles which are produced during the combustion are in solid form, whence they are fully recoverable at the outlet of the system. They can be regenerated using, for instance, a solar oven [3,4]. Consequently, a circular economy can be realized considering that the metal oxide produced can be collected and then reduced using clean primary energy/electricity.

During the last decade, metal flames were obtained by Lomba et al. [5] and by Julien et al. [6]. Then, a confined turbulent magnesium burner with swirl stabilization was designed by Garra et al. [7] and Laraqui et al. [8]. Metal fuels consisting of micron-sized iron particles are also promising alternative fuels [9].

During metal combustion in air, NOx are being produced. NOx species include nitrogen monoxide NO, nitrogen dioxide NO_2, nitrous oxide N_2O, nitrogen tetraoxide N_2O_4, nitrogen trioxide N_2O_3, nitrous acid HNO_2, and nitric acid HNO_3 [10–12]. To our knowledge, the first studies concerning NOx emissions generated during metal combustion were [7], [8] and [13]. The objective of the present study is therefore to reduce the knowledge gap concerning NOx production from the magnesium combustion and the impact of a dilution of the inlet air with nitrogen on these NOx emissions. There are three possible paths for nitrogen oxides formation: prompt NO, thermal NOx and fuel NOx [11,14]. For metal combustion, only thermal NOx are formed, through the combination of nitrogen from air with oxygen from air at high temperatures [13]. The Zeldovich mechanism is usually used to describe the formation of thermal NOx [15]. This reaction highly depends on temperature, oxygen content and residence time of the fuel in the flame. Nitrogen oxides cause acid rain which has a corrosive effect on materials as well as on the forest ecosystem and fresh water [16,17]. Moreover, NOx migrate into the troposphere and react with UV radiation, contributing to the formation of ground-level ozone [12,18]. N_2O causes an increase in greenhouse gases. In addition to these environmental impacts, nitrogen oxides have a negative effect on human health by impairing respiratory function. Nitric oxide enters the alveoli of the lungs and dissolves in the bloodstream, resulting in a decrease of the amount of oxygen carried by hemoglobin,

causing organs to suffer from a lack of oxygenation [10,11]. Numerous standards were introduced for the various sources of NOx emissions. For instance, Diesel vehicles must not emit more than 80 mgNOx/km driven [19]. French regulations established an upper limit of 40 µg/m^3 as an annual average not to be exceeded, with a target of a 63% reduction in NOx emissions at European level by 2030 compared to 2005 [20]. Two techniques can be implemented to contain the nitrogen oxides emissions from combustion systems. Primary techniques limit the formation of NOx in the combustion system. Secondary techniques consist of reducing the NOx formed with gas exhaust aftertreatment systems. Primary techniques allow lowering the combustion temperature and/or reducing the amount of injected oxygen to limit the rate of NOx production [11,14,21]. The most common of these techniques is fuel-staged combustion [14]. Its principle is to delay the injection of part of the fuel. Only a fraction of the fuel is injected at the entrance of the flame zone. This creates a fuel-poor zone in the flame where the temperature is consequently low. The remaining fuel is injected further down the flame. Thus, a second combustion zone is generated, which is fuel rich, and this limits the NOx formation. Combustion can also be staged by air injection. Indeed, when insufficient air flow is injected into the burner zone, combustion is therefore incomplete there. Additional air is then introduced downstream in the flame. The temperature is lower in the area where there is oxygen excess, which limits the NOx formation. Recycling the flue gases and diluting them in the flame can also lower the flame temperature. This recycling can be external or internal. External recycling or exhaust gas recirculation (EGR) consists to return the flue gases from the combustion system upstream of the burner where they are mixed with the primary air. This technique can reduce NOx formation by up to 60%. Internal recycling consists to circulate the flue gases near the burner [22,23]. Another technique consists to separate nitrogen from oxygen upstream of the combustion system. This oxy-combustion technique is currently used for stationary combustion sources, but it is not widely used for mobile sources as it is very costly. NOx reduction by gas re-burning is a secondary method which allows reducing nitrogen oxides with hydrocarbons in a slightly oxidizing environment [24]. The NOx formed in a first air-rich zone reacts in a second zone with hydrocarbons in an oxygen-poor atmosphere. The unburnt fuel then reacts with the NOx to reduce it. The unburned fuel is fully oxidized in a third zone where excess air is added. The efficiency of this pollution control system can be as high as 50%. Air staging and re-burning for NOx reduction appear to be the most suitable for metal combustion. These techniques enable the formation of NOx to be limited by intervening in the injection of air and fuel. They are to be favored in the first stage. Beside the primary techniques, the

secondary techniques allow reducing nitrogen oxides by using a reducing agent [25]. Secondary techniques should only be used when primary techniques do not provide sufficiently conclusive results. The only gaseous pollutants resulting from metal combustion are nitrogen oxides ($NOx=NO+NO_2$) [8]. Additionally, N_2O could also be produced. During the combustion of magnesium, the 2000 °C hot flame generates high levels of thermal NOx emissions [11]. These NOx levels must therefore be drastically reduced. The rates of NOx production depend on several factors, such as the temperature of the flame but also the oxygen availability in the flame and consequently the equivalence ratio. In the previous work [13], the NOx emissions from metal combustion were investigated using a turbulent magnesium burner where a swirl-stabilized flame was obtained in a combustion chamber. It was observed that the NOx emissions depend on the equivalence ratio and on the swirl. The NOx yielding exhibited a bell-shape curve versus the equivalence ratio, whatever the swirl. The NOx emissions never exceeded 7 g_{NOx}/kWh and it was expected to reduce them.

The present study aims at investigating the reduction of NOx emissions occurring during magnesium combustion in a pilot burner. Various techniques may be used to reduce the NOx emissions. They include two types of systems: pre-treatment and post-treatment such as Selective Catalytic Reduction (SCR) [26]. The objective of the present study is to reduce the NOx levels using a pre-treatment strategy which minimizes the NOx formation in the combustion system. For such a strategy, staged combustion is a very promising method which consist to delay the injection of a part of the fuel or of the oxidant in the combustion chamber, to separate the zone where the temperature is very high from the zone where the oxygen concentration is high [14,27]. Another method is the Exhaust Gas Recirculation (EGR), which consists to reinject part of the gases and fumes at the engine outlet in the burner where they are mixed with fresh air [22,23,28,29]. Considering the global mechanism proposed in [13] for NOx production in a magnesium flame, a relevant strategy for NOx abatement could be to reduce the flame temperature and the injected oxygen concentration. In the present study, the selected method simulates the EGR for NOx abatement. The confined combustion chamber with a stabilization by swirl is adapted for the characterization of NOx emissions and temperatures [8,13]. Nitrogen is mixed with air and injected upstream of the combustion chamber to simulate a dilution with the exhaust gases. For the dilution of hydrocarbons in a gasoline engine by recirculating gases or pure nitrogen, the dilution ratio cannot exceed 30%, because the dilution causes a significant unburned hydrocarbon rate and it is therefore necessary to find a compromise between the emissions of NOx and particles [22]. In the case of metal

combustion, such an issue does not appear and it is then possible to reach dilution ratios up to 50%. This study is therefore focused on the effect of the N_2 dilution on NOx emissions, as well as on the gas temperature in the combustion chamber, with dilution ratios of 0, 30 or 50%.

2. Experimental approach

2.1. Metal-air burner

The metal-air burner used was schematically described in [30]. Figure 1 gives a schematic representation of the pilot system.

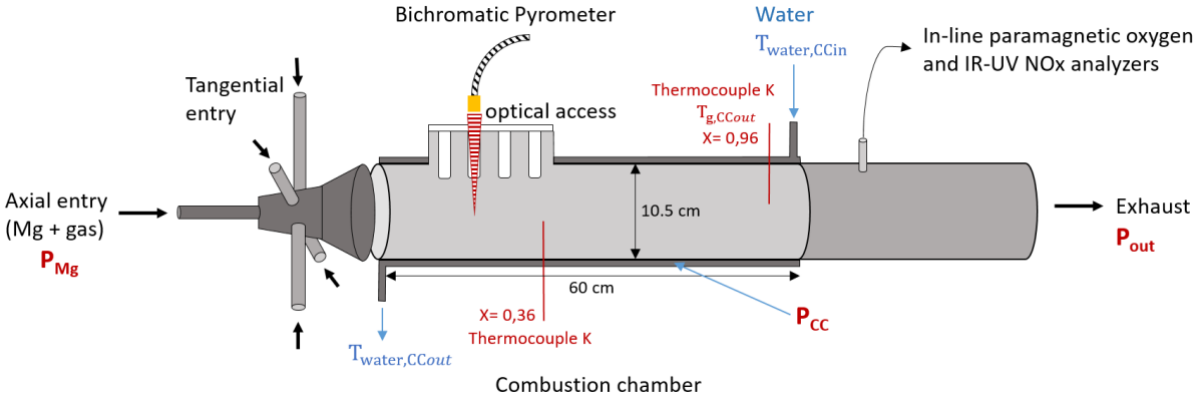

Fig. 1. Scheme of the pilot system.

The pilot system is composed of three main parts: an air and magnesium injection, a combustion chamber with an optical access for flame observation and an outflow duct for gas sampling and analysis. The combustion chamber is 60 cm long for an internal diameter of 10.5 cm. It consists in a cooled double-walled stainless-steel pipe. Cooling-water flows between the two concentric walls of the combustion chamber in the opposite direction of the gas flow for heat recovery purposes. The chamber opens onto a long outlet pipe, called the free exhaust, to avoid any pressure drop in the combustion chamber.

The fuel used is a magnesium powder with a purity greater than 99.8% and supplied by Carl Roth as CP20.2 reference. The particle size is characterized with a sifter RETSCH and it ranges from 50 to 70 µm. The generated aerosol of magnesium powder is injected into the chamber. Solid fuel injection was conducted with a PALAS BEG 1000 type B. This system allows a continuous and homogeneous injection of particles.

The reconstituted air and nitrogen flows are controlled before entering the chamber by solenoid valves and flow rates regulated by mass flowmeters. The injected airflow rate ranges between 2.3 and 8.6 $Nm^3.h^{-1}$. Nitrogen is additionally injected (between 0 and 4.3 $Nm^3.h^{-1}$), according to a given dilution rate to mimic exhaust gas recirculation with a dilution of the air by nitrogen.

The flame is stabilized with a swirl system where a secondary air is injected by four tangential inlets in the injection head. The swirl is characterized by its geometric swirl number S_g as already presented in [13]. The actual swirl number is approximately $0{,}24 \times S_g$. Only the ratio between axial mass flow rate and tangential mass flow rate affects the swirl number. In the present study, only one swirl condition is considered with $S_g = 7.3$.

The equivalence ratio is modified by increasing the flow of the magnesium injected at constant air supply injection. Equivalence ratio varies from 0.14 to 1.0. For such a range of equivalence ratio and depending on the dilution, the power supplied by the combustion varies between 6 and 23 kW.

2.2. Gas analyses and temperature measurements

A sample of the outlet gas flow is collected in the combustion chamber using a tube with three bored holes positioned perpendicularly to the flow. The holes are positioned back to the tube to avoid the holes plugging by the particles of magnesium oxide. The NO and NO_2 emissions are monitored using infrared and ultraviolet cells of X Stream Rosemount analysers. N_2O is measured using a Cascade analyser (Emerson Rosemount ct5400 continuous gas analyser). NOx are measured in ppm and are also expressed in $g.kWh^{-1}$ relating to the power dissipated by the combustion for comparison with NOx emission from gasoline engines.

The oxygen concentration at the outlet of the system is monitored using a paramagnetic X Stream Rosemount O_2 analyser, and expressed in %Vol.

The equivalence ratio can also be determined experimentally from:

$$\varphi = \frac{\%O_{2,i} - \%O_{2,f} \times \frac{100 - \%O_{2,i}}{100 - \%O_{2,f}}}{\%O_{2,i}}$$

where $\%O_{2,i}$ is the inlet oxygen mole fraction and $\%O_{2,f}$ is the outlet oxygen mole fraction.

The temperature of the gas in the chamber is measured using a type K thermocouple located in the flame at the normalized distance $x = L/L_{CC} = 0.36$, where L_{CC} is the total length of the combustion

chamber and L is the distance between the chamber entrance and the thermocouple. Additionally, a second type K thermocouple is positioned at the end of the chamber at x = 0.93. The thermocouples are gained Inconel 600 with an external diameter of 3 mm. The acquisition rate is 1 Hz. The gas temperatures reported are as measured by the thermocouples without any correction of the radiation. The position x = 0.36 corresponds to the heart of the flame, while the position x = 0.93 corresponds to the outlet of the combustion chamber. Moreover, the temperature of particles in the flame are measured using an IMPAC infrared ISR 12-LO bichromatic pyrometer (λ_1=800 nm, λ_2=1050 nm).

2.3. Dilution by N_2 of the injected air

An EGR (Exhaust Gas Recirculation) for reducing NOx emissions is simulated by injecting nitrogen into the carrier gas. This dilution with nitrogen is done without any modification of the volume of the carrier gas. Air and nitrogen are mixed together before being injected in the axial and tangential gas inlet. The air/nitrogen mixtures allow obtaining dilution ratios of 0, 30 and 50% nitrogen, the dilution rates being expressed as a volume percentage. Table 1 summarizes the experimental conditions for the different dilution ratios which are defined with respect to the total air flow.

Table 1: Experimental conditions for each dilution ratio.

Dilution ratio	Axial entry (Nm^3/h)	Tangential entry (Nm^3/h)	Mg mass flow rate (g/h)	Equivalence ratio	Thermal power (kW)
0%	3.6 Air	5 Air	950 – 3150	0.14 – 0.59	6 – 22
30%	2.52 Air + 1.08 N_2	2.1 Air + 1.5 N_2	1050 – 3300	0.22 – 0.92	7 – 23
50%	1.8 Air + 1.8 N_2	2.5 Air + 2.5 N_2	900 – 3000	0.28 – 1	6 – 21

Then the mixture is injected into the system; the primary gas flow rate including the magnesium particles is 3.6 Nm^3/h. The secondary/tangential gas flow rate is 5 Nm^3/h for the swirl number $S_g = 7.3$.

3. Results and Discussion

For metal combustion, only thermal NOx have to be considered, as fuel NOx and prompt NO are not relevant during the combustion of magnesium [13]. Zeldovich proposed a kinetic mechanism to simulate

193 the formation of thermal NOx [15]. O and N radicals from the dissociation of O_2 and N_2 allow NO
194 formation. NO formation is also strongly influenced by the temperature. As a consequence, among all
195 the experimental parameters investigated, oxygen concentration and temperatures are those which
196 should significantly influence the thermal NOx formation [15]. The particles and gas temperatures and
197 the oxygen mole fraction are first presented and discussed. The influences of the global equivalence
198 ratio and of the air dilution are analyzed for these experimental parameters. The NOx emissions versus
199 the equivalence ratio and dilution by N_2 are then presented and discussed, considering their
200 dependence on temperatures and oxygen mole fraction. At last, the results are analyzed through the
201 global mechanism for NOx formation presented in [13].
202
203 **3.1. Particle temperature**
204 The temperatures of the magnesia particles after recondensation are observed using a pyrometer.
205 Figure 2 gives the particles temperature as a function of the magnesium mass flow rate. The temperature
206 ranges between 1550 °C for a dilution of 50% to 2200 °C without any dilution.

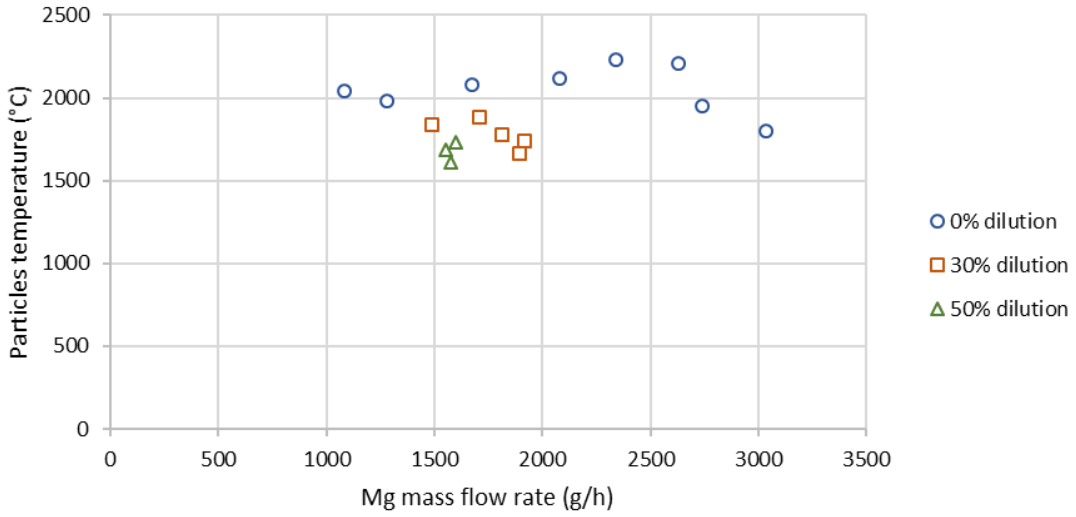

207
208 **Fig. 2.** Particles temperature versus the magnesium mass flow rate for the three dilution rates.
209
210 The particles temperature is not significantly influenced by the magnesium mass flow rate, but it
211 decreases when the dilution ratio increases.
212 Because the magnesium combustion takes place in a homogeneous phase, MgO is formed in the gas
213 phase and recondenses in the solid phase. The magnesia particles formed are initially at a temperature
214 of 3040 K which is the maximal temperature that solid magnesia can reach [31]. The bichromatic

pyrometer returns the temperature of a solid in the flame area. This solid cannot be the inner wall of the combustion chamber because it is cooled by water and therefore it remains at much lower temperatures than those measured by the pyrometer. It cannot also be magnesium because it is in vapor form at these temperatures. It is therefore surely the temperature of the magnesia.

The temperatures indicated in Fig. 2 are much lower than the theoretical value of 3000 K - which is close to the adiabatic flame temperature – obtained by Shoshin et al. [32] and Lim et al. [33]. Such a difference can be explained by the radiation and the convection heat losses in the combustion chamber that decrease the average flame temperature. These heat losses are induced by both the cooled walls of the combustion chamber and the optical access. They are enhanced by the turbulence in the swirled flame.

It is important to notice that the temperature of the particles decreases when the dilution factor increases. This could be explained by the depletion of oxygen in the flame when increasing the dilution ratio.

As the combustion rate of magnesium is a function of the O_2 concentration in the air-fuel mixture, when the O_2 mole fraction decreases, the combustion rate decreases and consequently the energy released by the combustion also decreases. Furthermore, nitrogen is a cold and non-reactive gas. A dilution with N_2 of the injected air necessarily leads to a decrease of the gas temperature in which the magnesia particles flow. Consequently, the magnesia particles cool faster in the gas. These two effects contribute to the decrease of the temperature of the magnesia particles.

3.2. Gas temperature

The thermocouples positioned at the normalized positions x = 0.36 and x = 0.93 allow to investigate the influence of the dilution on the gas temperature. The gas temperature does not significantly vary along the axis of the combustion chamber in the first half of the chamber [34]. The temperature obtained for x = 0.36 is a relevant indication of the average gas temperature in the flame zone. Moreover, the gas temperature increases during a time length of 200 s before reaching a plateau where only small fluctuations (lower than 20 °C) of the temperature versus time are observed.

Figure 3 presents the gas temperature at the position x = 0.36 as a function of the solid mass flow rate of the magnesium.

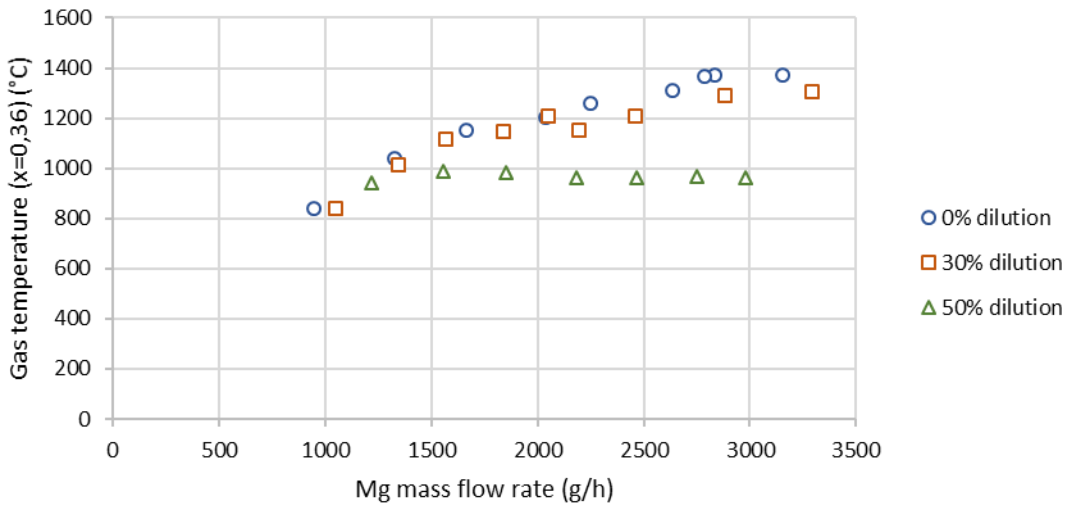

Fig. 3. Gas temperature at x=0.36 versus the magnesium mass flow rate for the three dilutions.

Until a solid flow rate of 1500 g/h, the temperature proportionally increases with this solid flow rate. Then, for higher solid flow rates, the temperature slowly increases for a nitrogen dilution of 0 and 30% or even does not increase for a dilution of 50%. The position of the flame is potentially shifted back in the chamber due to oxygen depletion when the dilution factor increases. Hence, the maximal heat release is also shifted back and consequently the gas temperature slowly increases at the position x = 0.36.

In addition, the gas temperature at x = 0.36 decreases with the nitrogen dilution. For a 50% dilution, the maximal gas temperature is 1000 °C to be compared to that 1400 °C obtained without any dilution. Such a decrease in the gas temperature when increasing the dilution ratio is well correlated with the decrease of the particle temperature in the same conditions as observed in Fig. 2.

Figure 4 depicts the gas temperatures as a function of the magnesium mass flow rate near the exit of the combustion chamber at x = 0.93.

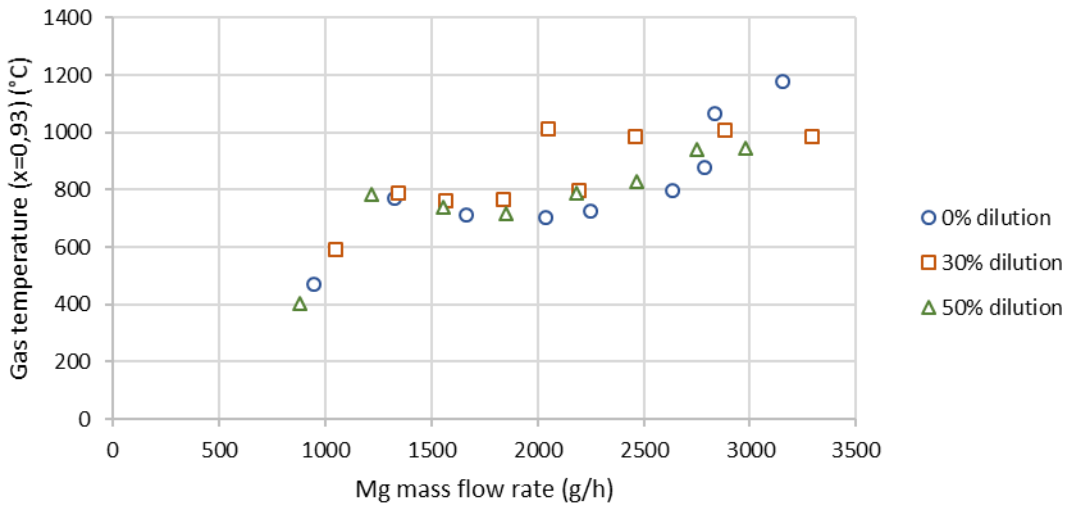

Fig. 4. Gas temperature at x = 0.93 versus the magnesium mass flow rate for the three dilutions.

The temperature ranges from 400 to 1200 °C, without any clear influence of the dilution on this temperature. The curves obtained for the three dilutions look quite similar. The temperature first increases when the magnesium mass flow rate increases from 800 to 1200 g/h. Then, a temperature plateau is observed for the magnesium flow rate ranging from 1200 to 2500 g/h. Finally, a slow increase of the temperature with the magnesium flow rate is observed. The two first stages are also observed for the temperature measured at x = 0.36, but with any clear influence of the dilution. Interestingly, the change of slope for the gas temperatures (at x = 0.36 and x = 0.93) appears for a magnesium mass flow rate of 1400 g/h. The position x = 0.93 is far from the flame zone which is located in the first half of the chamber, as previously shown by Laraqui et al. [30]. Consequently, the turbulence and the heat exchanges by thermal radiation and convection between the flame and the combustion chamber tend to homogenize the gas temperature from the middle to the exit of the chamber.

3.3. Heat Balance

A simplified heat balance is calculated, which accounts for the heat exchanges in the water-cooled combustion chamber and the heat exhausting the combustion chamber with the gas (N_2, O_2, NO and NO_2) and the solid (MgO). The heat exchange in the combustion chamber is calculated from both the inlet and outlet temperatures of the water circulating in the double wall exchanger and the water flowrate. The temperature of the gases and particles mixture leaving the combustion chamber is used to estimate the heat released at the chamber outflow.

The power dissipated by the combustion of the magnesium P_{Mg}, considering that it totally burns before leaving the chamber, the power recovered in the combustion chamber (P_{cc}) and that transported to the chamber outlet (P_{out}) are estimated using the following expressions:

$$P_{Mg} = \dot{m}_{Mg}.p_{Mg}$$

$$P_{CC} = \dot{m}_{water,chamber}.C_{p,water}.\left(T_{water,CCout} - T_{water,CCin}\right)$$

$$P_{out} = \dot{m}_{g,CCout}.C_{p,air}.\left(T_{g,CCout} - T_{g,ambient}\right) + \dot{m}_{MgO}.C_{p,MgO}.\left(T_{g,CCout} - T_{g,ambient}\right)$$

The injected power P_{Mg} is determined using the mass flow rate of magnesium and the specific energy of magnesium combustion p_{Mg} (24.8 kJ.kg^{-1}). The specific thermal capacities are denoted $C_{p,x}$ for the fluid or element x under consideration(expressed in kJ kg^{-1} K^{-1}). $T_{g,CCout}$ and $T_{g,ambient,I}$ are the gas temperatures measured with at the chamber outflow and the ambient temperature (°C). $T_{water,CCin}$ and $T_{water,CCout}$ are the temperatures of the water at the inlet and outlet of the cooling-water circuit (°C). $\dot{m}_{Mg}$, $\dot{m}_{water,chamber}$, $\dot{m}_{g,CCout}$ and $\dot{m}_{MgO}$ are the mass flow rate of Mg injected, cooling-water, gas, and MgO at the chamber (kg/s).

These balances are only indicative and comparative. They cannot be considered as absolute because after only 180 s thermal equilibrium is not reached in the system. P_{cc} and P_{out} are plotted versus P_{mg} in Fig. 5, for the three dilution ratios.

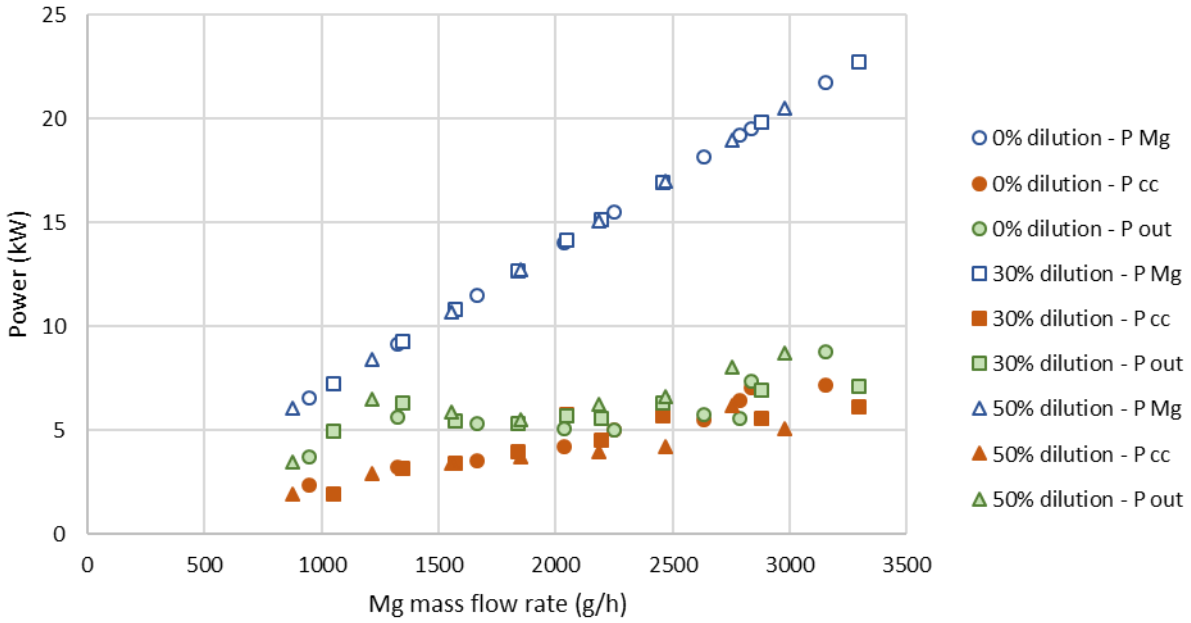

Fig. 5. Simplified heat balance for the three dilutions (0, 30 and 50%).

It appears that there is no significant effect of the dilution on the heat fluxes. This indicates that whatever the dilution, it does not impact the power recovery from the combustion.

As shown in Fig. 5, the sum of P_{cc} and P_{out} is equal to P_{Mg} for magnesium flow rates lower than 1500 g/h. This indicates that all the power delivered by the magnesium combustion is transmitted to the combustion chamber and carried by the gas and solid leaving the combustion chamber. For a magnesium flow rate greater than 1500 g/h, only a fraction of the power (approximately 66%) is transferred to the chamber on the one hand and leaves the chamber on the other hand. To explain such a behavior, it must be considered that the flame radiation is much less intense at low than at high equivalence ratio. Therefore, the fraction of the power transferred by radiation to the different parts of the burner, including the injection head, increases when the flow of injected magnesium increases. The power emitted by the flame radiation at the combustion chamber outlet is also not accounted for. They are not taken into account in the heat balance. This may explain the difference between the power dissipated by magnesium combustion and the power collected.

3.4. NOx emissions

Figure 6 depicts the NO and NO_2 mole fractions expressed in ppm as a function of the global equivalence ratio for the three tested dilutions.

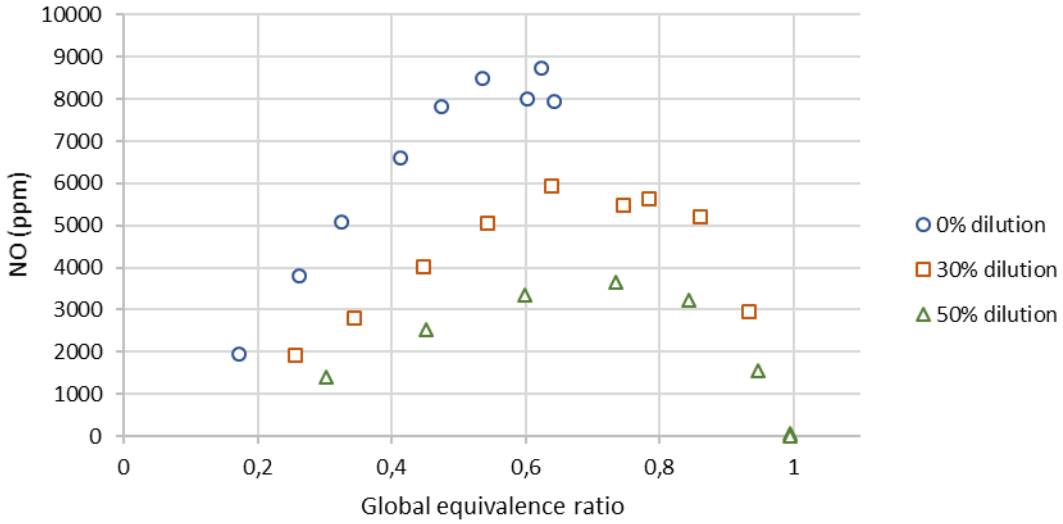

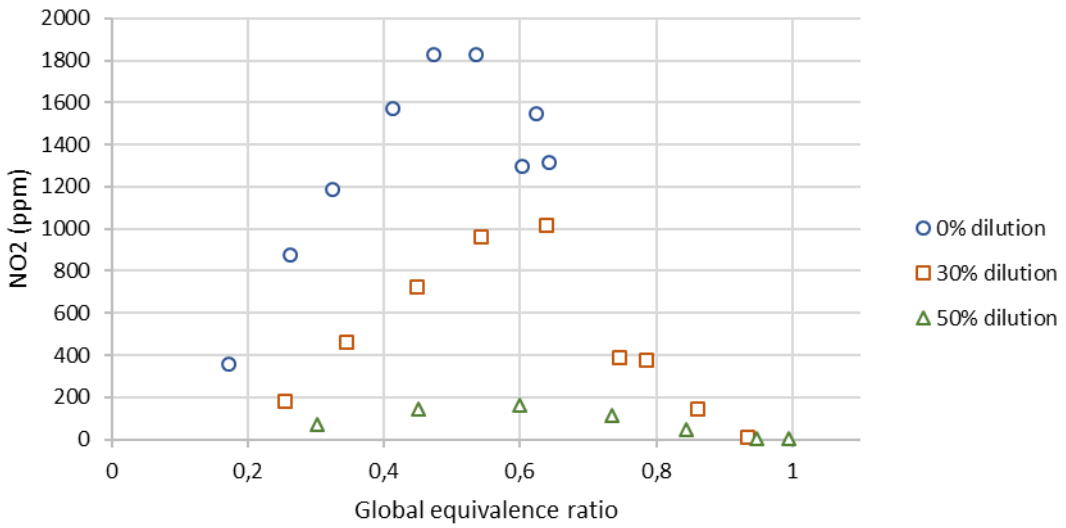

317

318 **Fig. 6.** NO and NO_2 emissions versus the global equivalence ratio for the three dilutions.

319

320 The NO and NO_2 mole fractions exhibit a parabolic shape curve. They first increase with the global
321 equivalence ratio until they reach a maximum. Then NOx emissions decrease. The maximal values for
322 NO mole fractions are 9000, 6000 and 3900 ppm for 0, 30 and 50% dilution, respectively. The effect of
323 the dilution ratio on NO_2 mole fractions is more pronounced. NO_2 emissions drastically reduce from 1800
324 to 100 ppm with a dilution ratio of 50%.
325 Considering the NOx emissions as a function of the global equivalence ratio according to the nitrogen
326 dilution rate, it first appears in Fig. 6 that the amount of NO formed is four times greater than the amount
327 of NO_2 formed. NO is formed before NO_2 with much faster kinetics. With a 50% dilution, the amount of
328 NO formed is divided by 2 and the amount of NO_2 formed is ten times less than without any dilution. In
329 addition, for a global equivalence ratio greater than or equal to 1 for a dilution rate of 50%, there is no
330 more oxygen to generate the formation of NOx, the levels of NO and NO_2 are both reduced to 0 ppm.
331 N_2O was measured for experiments performed with 0% dilution and a range of equivalence ratios from
332 0.57 to 0.97. No N_2O was observed whatever the experimental conditions tested.
333 The Mg particle burns in a micro-flame to produce MgO which recondenses. Increasing the Mg flow rate
334 increases the heat released by combustion and also increases the subsequent heat transfers by
335 convection and radiation between the MgO particles and the surrounding gas. This behavior can be
336 explained by the rise of the concentration of the MgO particles produced by combustion.
337 The residence time of the gas in the combustion chamber is approximately equal to 0.5 s. For such a
338 duration, a significant amount of thermal NOx can be produced only if the gas temperature is higher

than 2000 K. Such an assumption is well supported by a model based on the Zeldovich mechanism [15], and the associated kinetic parameters [35]. The duration of Mg oxidation is approximately equal to few milliseconds [36,37]. Hence, NOx formation surely occurs after Mg combustion is completed. It can occur in the gas phase in close contact with the surface of MgO particles where the gas temperature is higher than the mean gas temperature presented in Fig. 3.

According to the global mechanism for NOx formation proposed in [13], the NOx yielding increases when increasing the Mg mass flow rate. Indeed, the total contact area between MgO surface and the gas increases as MgO concentration rises. As shown in Fig. 3, the mean gas temperature increases as a function of the global equivalence ratio which is a consequence on the one hand of the power dissipated by Mg combustion and on another hand of the rise in MgO particles concentration.

For the highest equivalence ratios, the NOx mole fraction decreases due to the depletion of the available oxygen. The amount of oxygen becomes a limiting factor as shown in Fig. 7, causing a decrease in NOx emissions.

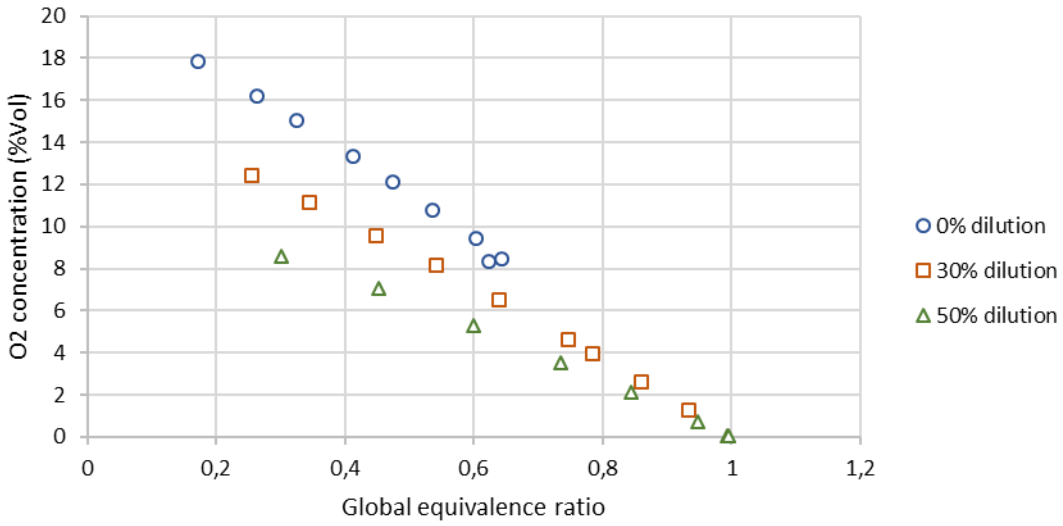

Fig. 7. Oxygen concentration versus the global equivalence ratio for the three dilutions.

As shown in Fig. 7, the oxygen mole fraction at the chamber outflow strongly decreases as the equivalence ratio increases. The oxygen defect for NOx formation results in the Mg oxidation which occurs before NOx formation. For a dilution of 50% and an equivalence ratio close to 1, oxygen concentration at the outflow is zero and this explain why no NOx are produced under such experimental conditions. All the oxygen available is consumed to burn Mg.

3.5. Efficiency of magnesium combustion versus N_2 dilution

All the injected metal powder Mg should be burnt and fully converted in MgO. A method to determine the completion of Mg oxidation was already presented by Garra et al. in [7]. This method is here used to determine the impact of the air dilution on the Mg oxidation. The combustion efficiencies of the solid samples collected at the entrance of the combustion chamber ($0.0 < x < 0.36$) and at the end of the combustion chamber ($x > 0.9$) are estimated.

For the particles collected at the chamber outflow, the combustion efficiency is close to 100%, whatever the tested experimental conditions. Hence, the dilution efficiency does not affect the Mg oxidation considering the overall chamber and there is no unburnt Mg at the chamber exit. Figure 8 depicts the results obtained for the different equivalence ratios and dilution levels for the particles collected at the entrance of the combustion chamber. The uncertainties are estimated from four experiments obtained from the same collected particles and represented by the error bars in Fig. 8.

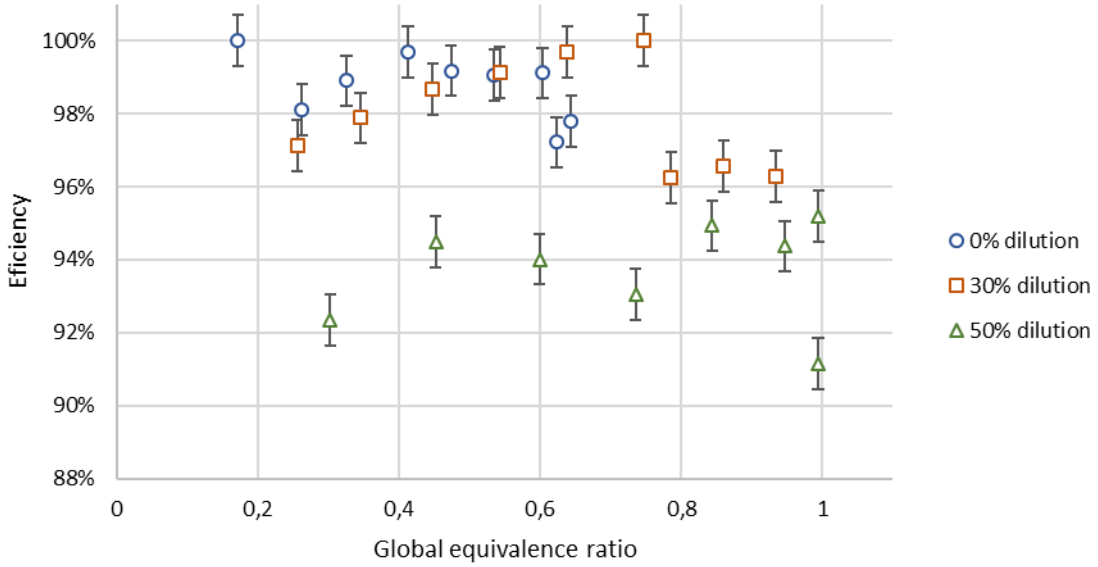

Fig. 8. Efficiency of the reaction at the entrance of the combustion chamber versus the global equivalence ratio for the three dilutions.

For the particles collected at the entrance of the combustion chamber, the combustion efficiency is very high for the 0 and 30% dilutions and for equivalence ratios smaller than 0.7. It significantly decreases (96%) for a dilution of 30% and for the highest equivalence ratio. For a dilution of 50%, the combustion efficiency is smaller, lying between 91 to 95%. This means that the oxygen concentration is not high

enough to promote the full combustion of Mg with a 50% dilution. Some Mg particles are partially oxidized and deposited on the chamber wall.

As the chamber is water-cooled, the wall temperature is too low for a slow oxidation [38] of the Mg particles deposited here. If the level of oxygen is too low to promote the full oxidation of Mg, it is clear that it is also too low for NOx formation.

Figure 8 gives the yield of Mg to MgO conversion for the particles collected at the beginning of the combustion chamber which approximately represent 20% of the mass of Mg/MgO collected. In the other part of the combustion chamber, in the cyclones and in the secondary heat exchanger, the particles collected are only MgO. They represent 80% of the mass of magnesia collected in the system. Thus, taking into account the whole system, the overall conversion is always higher than 98%, whatever the experimental conditions. The calculation of the equivalence ratio from the oxygen mole fractions at the inlet and outlet of the system can therefore be considered as close to reality.

The collected particles were observed by microscopy with a Keyence optical microscope already used by Moser et al. [38], see Fig. 9.

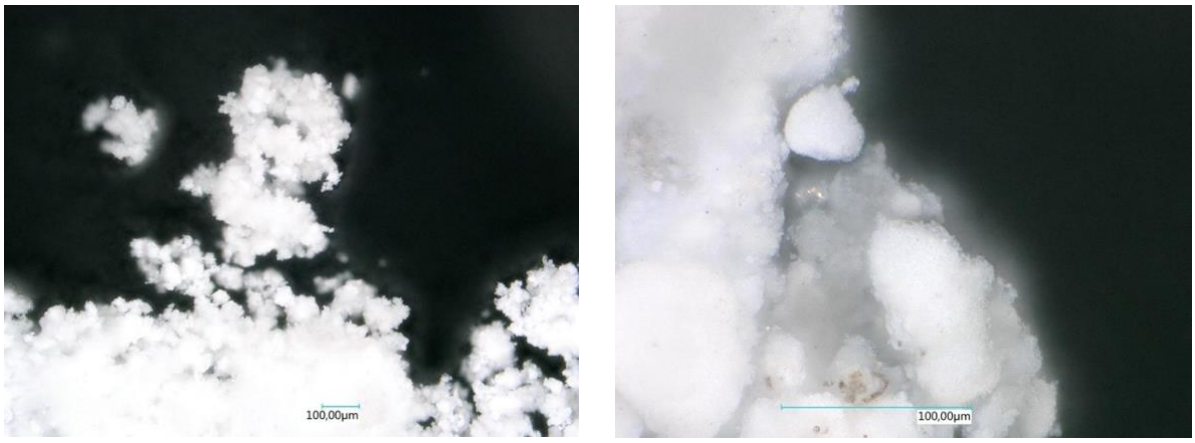

Fig. 9. Images of collected MgO (a) at the chamber outlet for 0% dilution and (b) at the chamber inlet obtained for 50% dilution.

As shown in Fig. 9.a, the MgO particles collected at the end of the combustion chamber for the experiments with 0% dilution are white aggregates of MgO. Such aggregates were already observed by Laraqui et al. [8]. The particles collected at the entrance of the combustion chamber for a 50% dilution (Fig. 9.b), exhibit some silvery metallic surface and appear to be not fully oxidised. The silvery metallic surfaces are characteristic of magnesium inclusion which are not observed on the magnesia sample

collected at the chamber outlet for undiluted combustion. Moser et al. also observed Mg particles partially oxidised in thermogravimetric experiments and Mg inclusions in MgO particles [38].

3.6. Comparison with NOx emissions of a gasoline engine

Figure 10 depicts the NOx emissions expressed in g/kWh as a function of the global equivalence ratio or of the Mg mass flow rate according to the dilution rate. The vertical error bars are calculated from the precision of the NOx analyser and the dissipated power. The horizontal error bars are calculated from the precision of the oxygen analyser. The maximal and minimal NOx emissions for a gasoline engine are also plotted for an easier comparison with a current gasoline engine as already presented for other experimental conditions by Laraqui et al. [8].

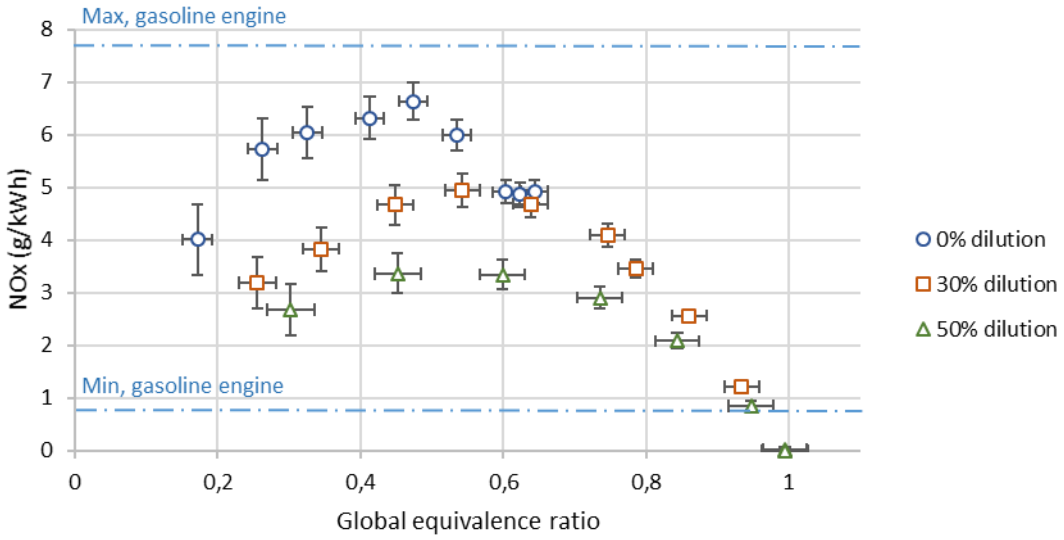

Fig. 10. NOx emission versus the global equivalence ratio for the three dilutions. Comparison with the NOx emissions from a gasoline engine.

Interestingly, the NOx yielding is lower than the maximal value emitted by gasoline engines and falls below the minimal value emitted by gasoline engines for a global equivalence ratio of 0.9 at a dilution of 50%. Moreover, as previously explained, there are no more NOx emitted at stoichiometry for a dilution of 50%, while this is not the case for gasoline engine, as prompt and fuel NOx are additionally produced. Such a result is very promising for the development of a technology using metal as energy carrier. The NOx yielding is minimized by an air dilution with nitrogen and the level of NOx are negligible for the highest values of equivalence ratio. 50% nitrogen dilution means that the injected gas is composed of a

mixture 50% air/50% nitrogen for a total gas flow rate similar to that injected for 0% dilution. Thus, half as much oxygen is brought into the burner. It is interesting to note that the NOx emissions appear in different ways if they are plotted against the injected magnesium flow rate, as presented in Fig. 11.

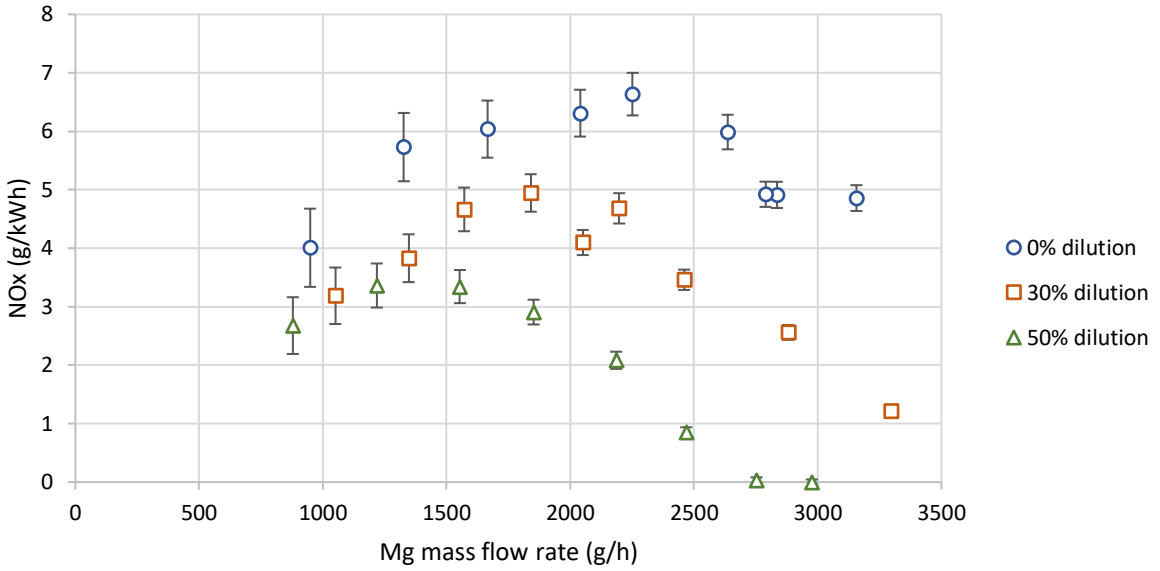

Fig. 11. NOx emissions versus the Mg mass flow rate ratio for the three dilutions.

Indeed, NOx emissions are not significantly affected by nitrogen dilution for the lowest magnesium injection rates. In this case, even though the oxygen fraction is lower as the nitrogen dilution rate increases, oxygen remains in excess in the combustion chamber as shown in Fig. 7. Thermal NOx can thus be formed in the gas phase in tight contact with magnesia. On the other hand, NOx emissions are significantly reduced with N_2 dilution for magnesium injection rates higher than 1500 g/h. In this case, there is certainly a lack of oxygen in the flame which limits the NOx production.

The maximal NOx emissions from the magnesium combustion is 6.55 g_{NOx}/kWh for 0% dilution and 3.25 g_{NOx}/kWh for 50% dilution. These maximal values are much higher than the amount currently emitted by coal power plant (from 0.2 to 0.4 g_{NOx}/kWh) or biomass power plant (from 0.2 to 0.7 g_{NOx}/kWh) [13]. However, for a 50% dilution ratio and an equivalence ratio closed to 1, the NOx emissions fall to 0 with the swirled-stabilized magnesium flame.

4. Conclusion

The study focused on the impact of N_2 dilution on the formation of thermal NOx during the combustion of magnesium in a swirled-stabilized turbulent flame. NO and NO_2 emissions versus the equivalence ratio exhibit a parabolic shape. No N_2O is detected. The NOx emissions ($NO+NO_2$) increase with the equivalence ratio until they reach a maximum. Such an increase is explained by the rise of the concentration of MgO particles in the combustion chamber. Indeed, NOx are produced in the gas phase in close contact with MgO particles where the temperature is high enough. After this maximum, NOx emissions decrease due to an oxygen depletion in the gas. Magnesium combustion reaction seems to be faster than NOx formation. The level of NOx never exceeded 7 g_{NOx}/kWh, which is lower than the maximal value of NOx emissions from a gasoline engine. A simulation of an exhaust gas recirculation with a nitrogen dilution (0, 30 and 50%) allows significantly reducing the NOx emissions, whatever the equivalence ratio. The maximal NOx emissions are shifted to higher equivalent ratios when increasing the dilution level and it decreases by a factor 2 with a dilution of 50%, for a constant value of the air-fuel ratio. The gas temperature in the flame decreases due to the N_2 dilution. Both such a temperature decrease and the O_2 depletion lead to limit the NOx formation. NOx emission tends to zero for an equivalent ratio of 1 and a nitrogen dilution of 50%.

CRediT authorship contribution statement

Adeline Andrieu: Methodology, Investigation, Writing – original draft. **Olivier Allgaier**: Investigation. **Gontrand Leyssens**: Conceptualization, Validation, Supervision. **Cornelius Schönnenbeck**: Conceptualization, Validation, Supervision. **Jean-François Brilhac**: Conceptualization, Validation, Supervision, Writing – original draft, Writing – review & editing, Project administration. **Alain Brillard**: Validation, Writing – original draft, Writing – review & editing, Project administration. **Valérie Tschamber**: Project supervision.

Declaration of Competing Interest

The authors declare that they have no known competing financial interests or personal relationships that could have appeared to influence the work reported in this paper.

Acknowledgment

Financial support from the French National Research Agency (convention ANR- 18-CE05-0040) is gratefully acknowledged.

References

[1] Bergthorson JM, Goroshin S, Soo MJ, Julien P, Palecka J, Frost DL, et al. Direct combustion of recyclable metal fuels for zero-carbon heat and power. Applied Energy 2015;160:368–82. https://doi.org/10.1016/j.apenergy.2015.09.037.

[2] Bergthorson JM, Yavor Y, Palecka J, Georges W, Soo M, Vickery J, et al. Metal-water combustion for clean propulsion and power generation. Applied Energy 2017;186:13–27. https://doi.org/10.1016/j.apenergy.2016.10.033.

[3] Julien P, Bergthorson JM. Enabling the metal fuel economy: green recycling of metal fuels. Sustainable Energy Fuels 2017;1:615–25. https://doi.org/10.1039/C7SE00004A.

[4] Puig J, Balat-Pichelin M. Production of metallic nanopowders (Mg, Al) by solar carbothermal reduction of their oxides at low pressure. Journal of Magnesium and Alloys 2016;4:140–50. https://doi.org/10.1016/j.jma.2016.05.003.

[5] Lomba R, Laboureur P, Dumand C, Chauveau C, Halter F. Determination of aluminum-air burning velocities using PIV and Laser sheet tomography. Proceedings of the Combustion Institute 2019;37:3143–50. https://doi.org/10.1016/j.proci.2018.07.013.

[6] Julien P, Whiteley S, Goroshin S, Soo MJ, Frost DL, Bergthorson JM. Flame structure and particle-combustion regimes in premixed methane–iron–air suspensions. Proceedings of the Combustion Institute 2015;35:2431–8. https://doi.org/10.1016/j.proci.2014.05.003.

[7] Garra P, Leyssens G, Allgaier O, Schönnenbeck C, Tschamber V, Brilhac J-F, et al. Magnesium/air combustion at pilot scale and subsequent PM and NOx emissions. Applied Energy 2017;189:578–87. https://doi.org/10.1016/j.apenergy.2016.12.069.

[8] Laraqui D, Allgaier O, Schönnenbeck C, Leyssens G, Brilhac J-F, Lomba R, et al. Experimental study of a confined premixed metal combustor: Metal flame stabilization dynamics and nitrogen oxides production. Proceedings of the Combustion Institute 2019;37:3175–84. https://doi.org/10.1016/j.proci.2018.07.018.

[9] Ning D, Shoshin Y, van Oijen JA, Finotello G, de Goey LPH. Critical temperature for nanoparticle cloud formation during combustion of single micron-sized iron particle. Combustion and Flame 2022;244:112296. https://doi.org/10.1016/j.combustflame.2022.112296.

[10] Définition, sources d'émission et impacts. ADEME n.d. https://www.ademe.fr/entreprises-monde-agricole/reduire-impacts/reduire-emissions-polluants/dossier/oxydes-dazote-nox/definition-sources-demission-impacts (accessed December 19, 2019).

[11] Thomas D. NO (oxydes d'azote). Ref : TIP800WEB - "Environnement" 2009. https://www.techniques-ingenieur.fr/base-documentaire/42600210-traitements-de-l-air/download/g1805/no-oxydes-d-azote.html (accessed December 5, 2019).

[12] Clean Air Technology Center (CATC). Nitrogen Oxides (NOx), Why and How They are Controlled n.d.:57.

[13] Andrieu A, Allgaier O, Leyssens G, Schönnenbeck C, Brilhac J-F. NOx emissions in a swirled-stabilized magnesium flame. Fuel 2022;321:124011. https://doi.org/10.1016/j.fuel.2022.124011.

[14] Jacubowiez I. Dénitrification des gaz de combustion 1998:20.

[15] Zeldovich Y. Oxidation of Nitrogen in Combustion. Publishing House of the Acad of Sciences of USSR; 1947.

[16] Pollution de l'air : origines, situation et impacts. Ministère de la Transition écologique et solidaire n.d. http://www.ecologique-solidaire.gouv.fr/pollution-lair-origines-situation-et-impacts (accessed December 19, 2019).

[17] Effets des NOx sur la santé et l'environnement n.d. http://environnement.public.lu/fr/loft/air/Polluants_atmospheriques/les_oxydes_d_azote_NOx/effets-NOx.html (accessed December 19, 2019).

[18] Ray M-C. NOx. Futura n.d. https://www.futura-sciences.com/planete/definitions/pollution-nox-17036/ (accessed December 19, 2019).

[19] Émissions de particules et de NOx par les véhicules routiers – ADEME n.d. https://www.ademe.fr/emissions-particules-nox-vehicules-routiers (accessed January 7, 2020).

[20] Directive (EU) 2016/2284 du Parlement européen et du Conseil du 14 décembre 2016 concernant la réduction des émissions nationales de certains polluants atmosphériques, modifiant la directive 2003/35/CE et abrogeant la directive 2001/81/CE (Texte présentant de l'intérêt pour l'EEE). vol. OJ L. 2016.

[21] Bradley MJ, Jones BM. Reducing Global NOx Emissions: Developing Advanced Energy and Transportation Technologies. Ambi 2002;31:141–9. https://doi.org/10.1579/0044-7447-31.2.141.

[22] Wang Z, Zhou S, Feng Y, Zhu Y. Research of NOx reduction on a low-speed two-stroke marine diesel engine by using EGR (exhaust gas recirculation)–CB (cylinder bypass) and EGB (exhaust gas bypass). International Journal of Hydrogen Energy 2017;42:19337–45. https://doi.org/10.1016/j.ijhydene.2017.06.009.

[23] Lipardi ACA, Versailles P, Watson GMG, Bourque G, Bergthorson JM. Experimental and numerical study on NOx formation in CH4–air mixtures diluted with exhaust gas components. Combustion and Flame 2017;179:325–37. https://doi.org/10.1016/j.combustflame.2017.02.009.

[24] Smoot LD, Hill SC, Xu H. NOx control through reburning1This mini-review paper was presented, together with a series of other review papers, at the Tenth Annual Technical Conference of the Advanced Combustion Engineering Research Center, held in Salt Lake City, Utah, in March 1997.1. Progress in Energy and Combustion Science 1998;24:385–408. https://doi.org/10.1016/S0360-1285(97)00022-1.

[25] Réduction des NOx - traitement des fumées : réduction sélective non catalytique ou catalytique | Atee - Association Technique Energie Environnement n.d. http://atee.fr/energie-plus-magazine/r%C3%A9duction-des-nox-traitement-des-fum%C3%A9es-r%C3%A9duction-s%C3%A9lective-non-catalytique-ou (accessed January 13, 2020).

[26] Liu Z, Woo SI. Recent Advances in Catalytic DeNOX Science and Technology. Catalysis Reviews 2006;48:43–89. https://doi.org/10.1080/01614940500439891.

[27] Shihadeh AL, Toqan MA, Beer JM, Lewis PF, Teare JD, Jimenez JL, et al. Low NO{sub x} emission from aerodynamically staged oil-air turbulent diffusion flames 1994.

[28] Maiboom A, Tauzia X, Hétet J-F. Experimental study of various effects of exhaust gas recirculation (EGR) on combustion and emissions of an automotive direct injection diesel engine. Energy 2008;33:22–34. https://doi.org/10.1016/j.energy.2007.08.010.

[29] Kuroda H, Nakajima Y, Sugihara K, Takagi Y, Muranaka S. The Fast Burn with Heavy EGR, New Approach for Low NO x and Improved Fuel Economy. SAE Transactions 1978;87:1–15.

[30] Laraqui D, Leyssens G, Schonnenbeck C, Allgaier O, Lomba R, Dumand C, et al. Heat recovery and metal oxide particles trapping in a power generation system using a swirl-stabilized metal-air burner. Applied Energy 2020;264:114691. https://doi.org/10.1016/j.apenergy.2020.114691.

[31] Glassman I, Yetter R. Combustion Ed. 4. Elsevier Science; 2008.

[32] Shoshin YL, Dreizin E. Particle combustion rates in premixed flames of polydisperse metal - Air aerosols. Combustion and Flame 2003;133:275–87. https://doi.org/10.1016/S0010-2180(02)00571-0.

[33] Lim J, Lee S, Yoon W. A comparative study of the ignition and burning characteristics of afterburning aluminum and magnesium particles. J MECH SCI TECHNOL 2014;28:4291–300. https://doi.org/10.1007/s12206-014-0943-3.

[34] Andrieu A. Combustion de métaux dans un brûleur turbulent: étude de la stabilisation de la flamme et réduction des polluants, PhD thesis,. Université de Haute-Alsace, 2022.

[35] Hanson RK, Salimian S. Survey of Rate Constants in the N/H/O System. In: Gardiner WC, editor. Combustion Chemistry, New York, NY: Springer; 1984, p. 361–421. https://doi.org/10.1007/978-1-4684-0186-8_6.

[36] Cassel HM, Liebman I. Combustion of magnesium particles I. Combustion and Flame 1962;6:153–6. https://doi.org/10.1016/0010-2180(62)90084-6.

[37] Shevtsov VI, Fursov VP, Stesik LN. Mechanism for combustion of isolated magnesium particles. Combust Explos Shock Waves 1976;12:758–63. https://doi.org/10.1007/BF00740747.

[38] Moser G, Schönnenbeck C, Tschamber V, Brillard A, Brilhac J-F. Experimentation and kinetic modeling of low-temperature oxidation of magnesium particles for the production of energy with low environmental impact. Combustion and Flame 2021;230:111419. https://doi.org/10.1016/j.combustflame.2021.111419.